Tailings Liquefaction Analysis Using Strength Ratios and SPT/CPT Results

W. Pirete, R.C. Gomes

Abstract. Tailings dams constructed using the upstream method generally have relatively low- density materials with a high degree of saturation. Such conditions can generate the phenomena of liquefaction, which is potentially critical in slurry tailings disposal systems. Slope stability analyses involving liquefied soil require that the shear resistance of the softened soil be estimated and then, a good practical alternative is back-analyzed with field case studies involving slope failures, using commonly SPT and CPT results. The Olson (2001) and Olson & Stark (2003b) liquefaction analysis methodology based on strength ratios, included in this approach, is comprised of three stages: (i) liquefaction susceptibility analysis; (ii) triggering analysis; and (iii) post-triggering - flow failure stability analysis. In this paper, this approach was applied for stability assessments to verify liquefaction potential in an upstream tailings dam built by the hydraulic fill technique and located in the *Quadrilátero Ferrífero* (Iron Quadrangle) region, southeastern of Brazil. The results ratified the safety condition of the impoundment although they have demonstrated that the tailings tend to exhibit contractile behavior during shear, indicating liquefaction susceptibility.

Keywords: tailings, liquefaction, strength ratio, SPT tests, CPT tests.

1. Introduction

In general, liquefaction can be understood as the phenomenon of the strain-softening of contractive, saturated and cohesionless soils during undrained shear and can be triggered by static or seismic undrained loading or undrained deformation under constant load. This behavior results in a liquefaction flow failure in the field if the static shear stress is greater than the liquefied (or steady state) shear strength. The liquefied shear strength is defined as the shear strength mobilized by large deformation after liquefaction is triggered in saturated, contractive and cohesionless soils. In addition, this condition has also been referred to as undrained residual shear strength (Seed, 1987), undrained steady state shear strength (Poulos *et al.*, 1985), and undrained critical shear strength (Stark & Mesri, 1992).

Although 'liquefaction' is commonly used to describe all failure mechanisms resulting from the build-up of pore pressures during the undrained cyclic shear of saturated cohesionless soils, some ground failures attributed to 'soil liquefaction' are more correctly ascribed to 'cyclic mobility', since it results in limited soil deformations (Gomes, 2010). Liquefaction can occur even in unsaturated soils, with a sufficient saturation degree to induce contraction associated to water dissipation instead of air (Yoshimi *et al.*, 1989; Aubertin *et al.*, 2003). Laboratory tests have confirmed the possibility of liquefaction even in materials with a saturation degree of 80% (Martin, 1999).

Except for the fine fraction of ore bodies with substantial mineral clay content, tailings are usually cohesionless materials, conventionally deposited in the form of slurry by hydraulic fill techniques in raised embankments. Raised embankments can be constructed using upstream, downstream, or centerline methods (Vick, 1990). Each one of the structures is constructed in stages, with constructing material and fill capacity increasing incrementally with each successive raising.

Upstream construction, the most economical method, begins with a starter dam constructed at the downstream toe. The tailings are discharged peripherally from the crest of the starter dam using spigots or cyclones. This deposition develops a dike and wide beach area composed of coarse material that becomes the foundation of the next dike. These dikes can be built with borrow fill, or tailings can be excavated from the beach and placed by dragline or bulldozer. The single most important criteria for the application of the upstream construction method is that the tailings beach must form a competent foundation for the support of the next dike.

The phreatic surface exerts a large degree of control over the stability of the structure, under both static and seismic loading conditions. The primary method of maintaining a low phreatic surface near the embankment face is to guarantee an elevated hydraulic conductivity of the deposit in the direction of flow. There are four factors influencing the phreatic surface location: the permeability of the foundation relative to the tailings; the degree of grain-size segregation; the lateral permeability variation within the deposit; and the location of the reservoir relative to the embankment crest. Only the reservoir limit can be controlled through operational practices, by maintaining a large tail-

Soils and Rocks, São Paulo, 36(1): 37-53, January-April, 2013.

37

ings beach extension. Water control and management are the most critical elements of tailings dam design and operation.

Tailings dams constructed using the upstream method generally have relatively low- density materials with a high degree of saturation. On the other hand, the wide ranges in the initial void ratio, together with the structure of tailings deposits, imply that predictions of the in situ undrained strength for these materials are highly uncertain. Such conditions generate the phenomena of liquefaction, which is potentially critical in these slurry tailings disposal systems (Troncoso & Verdugo, 1985; Vick, 1990; ICOLD & UNEP, 2001; Bray *et al.*, 2004).

Although such systems are very susceptible to liquefaction mechanisms under dynamic loading (Kramer, 1996; Seid-Karbasi & Byrne, 2004), mine tailings impoundments have demonstrated that more static liquefaction events than seismic induced events occur in function of the loading rates (Ishihara *et al.*, 1990; Davies *et al.*, 2002; Olson, 2006; Byrne, 2008). In fact, if the loading rate is quick enough or if the tailings present sufficiently low relative hydraulic conductivity, shear-induced pore pressures are generated and, as a result, effective stresses are reduced and both stiffness and shear strength degrade. In tailings impoundments, particularly upstream tailings dams, potential static liquefaction triggers include (Davies *et al.*, 2002):

- Increased pore pressures induced by an increase in the piezometric surface, and/or change of pore pressure conditions from below hydrostatic to hydrostatic, or to higher than hydrostatic.
- Excessive rate of loading due to the rapid rise of the impoundment;
- Removal of toe support from an overtopping event;
- Foundation movements, rapid enough to generate undrained loading in tailings susceptible to spontaneous collapse.

Several procedures have been proposed for estimating the liquefaction potential or susceptibility of soils or tailings. These techniques include commonly experimental procedures based on lab tests results (Poulos *et al.*, 1985; Sladen *et al.*, 1985; Ishihara, 1993; Yamamuro & Lade, 1997, Gomes *et al.*, 2002; Olson & Stark, 2003a; Pereira, 2005).

To determine liquefied shear strength, methodologies based on laboratory tests require high-quality samples and the adoption of correction factors to compensate for potential volume variations that occur during sampling and testing (Poulos *et al.*, 1985; Ishihara, 1993; Idriss and Boulanger, 2007). This is due to the fact that any errors in determining the levels of voids in situ may result in large differences in the results, since the position of the steady state line is influenced by the sample preparation technique, by the shear mode and by the effective confining stresses.

Thus, greater emphasis has been given to empirical methods that correlate corrected values of resistance from SPT and CPT tests with liquefaction failure results from case histories that were back-analyzed (Seed *et al.*, 1985; Stark and Mesri, 1992; Ishihara, 1993; Olson 2001, Olson and Stark, 2003b; Idriss and Boulanger, 2007a). These studies are based on classical concepts of soil mechanics, such as critical void ratio, steady state line, peak strength and liquefied shear strength (Casagrande, 1975; Castro, 1975; Poulos *et al.*, 1985; Kramer, 1996; Olson, 2001).

In this context, the estimated values of shear strength in these analyses constitute parameters that are more representative than those obtained in laboratory testing, because they embody the complex reality of actual deposits, the physical interaction of different materials and even the failure kinetics processes. However, there remain some uncertainties that affect the estimated values of resistance, mainly due to difficulties in establishing the rigid boundaries of the liquefaction zone, the location of the sliding surfaces and the drainage and pore pressures conditions mobilized during the flow.

The liquefaction methodology proposed by Olson (2001) consists of a triggering analysis based on field tests and does not require a suite of laboratory tests or correction procedures. The author collected thirty-three case histories of liquefaction flow failures that were back-analyzed to evaluate the yield and liquefied shear strength. Relationships between yield strength ratio and corrected SPT and CPT resistance were developed for use in liquefaction triggering analyses and also, those between liquefied strength ratio and corrected SPT and CPT resistance were developed for use in post-triggering stability analyses.

The general principles and technical basis of this methodology are set out below, covering three primary analyses: (i) liquefaction susceptibility analysis; (ii) triggering analysis; and (iii) post-triggering - flow failure stability analysis (Olson, 2001; Olson & Stark, 2003b).

## 2. Liquefaction Resistance Based on SPT and CPT Tests

2.1. Liquefaction susceptibility

The first step of a tailings liquefaction analysis is to determine whether a tailings deposit is in a contractive state, *i.e.*, susceptible to undrained strain-softening behavior and flow failure. These states are established based on correlations between overburden-stress normalized penetration resistance (either CPT tip resistance or SPT blow count - a measure of soil density) and vertical effective stress (pre-failure condition). The corrected blowcount, $(N_1)_{60}$, is defined as the SPT blowcount at a vertical effective stress of 100 kPa and an energy level equal to 60% of the theoretical free-fall hammer energy. The correct cone tip resistance, q_{c1}, is expressed as $q_{c1} = q_c \cdot C_q$, where C_q is the CPT based overburden correction factor.

Figures 1 and 2 respectively present SPT and CPT values based on flow failure susceptibility relationships

38

Soils and Rocks, São Paulo, 36(1): 37-53, January-April, 2013.
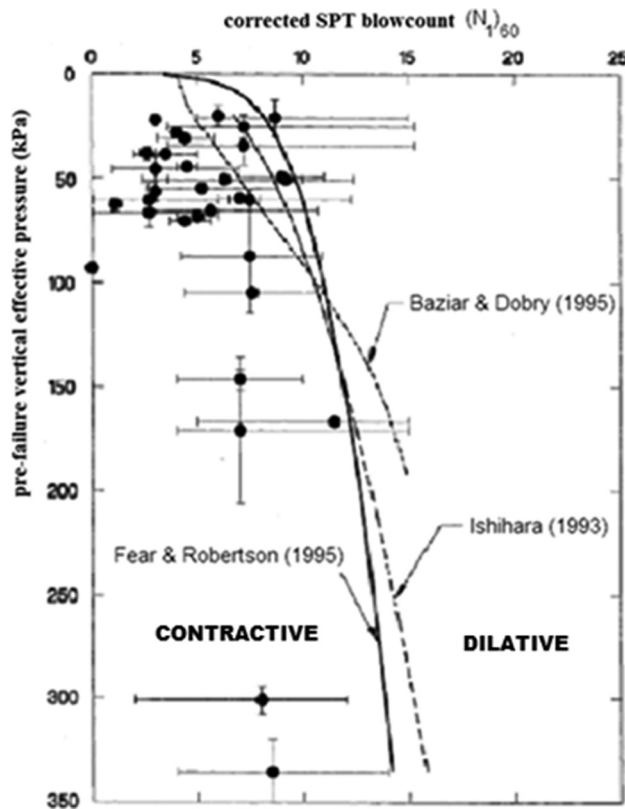
Figure 1 - Relationships separating contractive from dilative conditions using flow failure case histories and corrected SPT blowcount values (Olson, 2001).
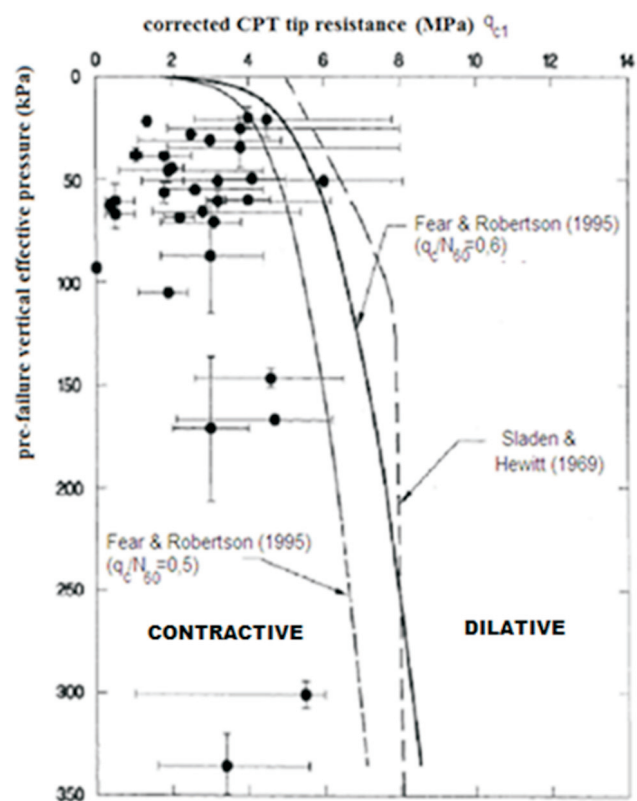
Figure 2 - Relationships separating contractive from dilative conditions using flow failure case histories and corrected CPT tip resistance values (Olson, 2001).

from literature with case history data. Based on the agreement with theory, laboratory results, and field case histories, the Fear & Robertson (1995) boundary was recommended by the author (Olson, 2001) to delineate field conditions susceptible and not to flow failure in both cases.

In a specific design, records of q_{c1} and/or $(N_1)_{60}$ should be plotted against vertical effective stress, including the recommended relationship.The liquefaction susceptibility analysis involves two hypotheses:

- Tailings exhibit <u>dilative behavior</u>: tailings liquefaction susceptibility <u>is unlikely</u> and the analysis is completed;
- Tailings exhibit <u>contractive behavior</u>: tailings liquefaction susceptibility <u>is likely</u> and this analysis should be complemented by the triggering analysis and post-triggering - flow failure stability analysis.

2.2. Triggering analysis

For tailings that show to be contractive under shear from the previous analysis, a liquefaction triggering analysis is performed to determine whether the imposed loading conditions (in these analyses, static loading) are sufficient to cause the soil to exceed its yield strength ratio and trigger liquefaction. This additional analysis is an extension of a traditional slope stability analysis typically performed with commercial software, and can be readily facilitated with the

use of a spreadsheet and data obtained from the slope stability software.

The liquefaction triggering analysis is based on a limit equilibrium stability back-analysis (considering non-circular and circular surfaces), from the pre-failure geometry of the slope to estimate the average static shear stress (τ_d) in soils susceptible to liquefaction. A single value of shear strength is assumed, then, for soils susceptible to liquefaction and this resistance is continually changed to obtain FS = 1.0 and the corresponding critical surface rupture.

The critical failure surface is subdivided into a number of segments (10 to 15 segments are recommended) and is determined the weighted effective vertical stress, σ'_{v0} (average value) along the critical failure surface (within the zone of soil susceptible to liquefaction), and calculate the average static shear stress ratio τ_d/σ'_{v0}. If applicable, average seismic shear stresses (and other shear stresses applied to each segment of the yield failure surface) are evaluated using complementary analyses (Olson & Stark, 2003b).

In addition, yield strength ratios ($s_{u(yield)}/\sigma'_{v0}$), appropriate for each slice of the critical failure surface, are estimated based on corrected SPT and/or CPT penetration resistance values. In this analysis step, a desired level of conservatism can be incorporated by using a penetration resistance smaller than the mean value, or by selecting a yield

strength ratio higher or lower than the mean value. In this manner, it is possible determine the liquefaction potential in each segment using a safety factor against liquefaction triggering that comprise two hypotheses:

• Segments with $(FS)_{triggering} > 1.0$ are unlikely to liquefy (post-triggering stability analysis is unnecessary if all segments have $(FS)_{triggering} > 1.0$);

• Segments with $(FS)_{triggering} \leq 1.0$ are likely to liquefy and these segments should be assigned the liquefied shear strength for a post-triggering stability analysis (segments with $(FS)_{triggering} > 1.0$ should be assigned their yield shear strength for a post-triggering stability analysis).

The authors recommend that both the critical circular and noncircular failure surfaces be analyzed, varying in depth and location within the zones of contractive tailings. If the circular and noncircular failure surfaces cross the zones of contractive soil at about the same location and depth, it is recommended that one or two additional potential failure surfaces that cross these zones at different locations be analyzed.

2.3. Post-triggering - Flow failure stability analysis

After the characterization phase of the liquefaction triggering, a post-triggering stability analysis of the structure, using the pre-failure geometry, must be conducted to determine whether the static shear forces are greater than the available shear resistance, including the liquefied shear strength. In this case, the liquefied shear strength ratio $(s_{u(liq)}/\sigma'_{v0})$, appropriate for each slice of the critical failure surface, is determined based on corrected SPT and/or CPT penetration resistance values. Appropriate values of liquefied shear strength are estimated (using the value of σ'_{v0} for the segment) and assigned to the segments of the critical failure surface predicted to liquefy from the triggering analysis. Fully mobilized drained or undrained shear strengths are assigned to the non liquefied soils.

This analysis should be conducted for all of the potential failure surfaces that were examined in the triggering analysis. Another level of conservatism can be incorporated by using a penetration resistance smaller than the mean value, or by selecting a yield strength ratio higher or lower than the mean value. The post-triggering analysis results comprise two hypotheses:

• Safety factor against flow failure $(FS)_{flow} \leq 1.0$: flow failure is predicted to occur; control procedures should be adopted to increase impoundment safety;

• Safety factor against flow failure $(FS)_{flow}$ such that $1.0 < (FS)_{flow} \leq 1.1$: flow failure has little possibility to occur, but some deformation is likely (the segments of the failure surface with $1.0 < (FS)_{flow} \leq 1.1$ should be reassigned their liquefied shear strength).

The post-triggering stability analysis should be repeated with the new segment shear strengths to determine a new $(FS)_{flow}$. This accounts for the potential for deforma-

tion-induced liquefaction and progressive failure of the structure. The minimum $(FS)_{flow}$ will be determined when liquefaction is triggered in all zones of contractive soil and assigned their liquefied shear strengths for the flow failure stability analysis.

Post-liquefaction behavior is characterized by a very complex process involving dissipation of excess pore water pressure, sedimentation, solidification and re-consolidation of the liquefied tailings resulting in large settlements of the deposit. If the results of the post-triggering stability analysis indicate $(FS)_{flow}$ below unity, then mitigation strategies are required. In tailings dams constructed using the upstream method, this approach consists basically in the maintenance of a large tailings beach extension, with adoption of rigid operational procedures of water control. For segments with $(FS)_{triggering} > 1.0$, the post-triggering analysis can be conducted in a similar way using yield shear strength.

Nevertheless, the reliability of any liquefaction evaluation depends directly on the quality of the site characterization, including mainly the quality of the in situ and/or laboratory test data.

Furthermore, it is often the synthesis of findings from several different procedures that provides the most insight and confidence in making final decisions. For this reason, the practice of using different testing methodologies constitutes the best approach for liquefaction analyses in tailings impoundments, so that semi-empirical methodologies based on back-analysis of field case studies involving slope failures are strongly recommended.

3. Case History: Córrego do Feijão Mine - Dam I

The liquefaction analysis methodology using the strength ratio approach proposed by Olson (2001) and Olson & Stark (2003b) was applied to a tailings impoundment located in the so-called *Quadrilátero Ferrífero* (Iron Quadrangle) region, located in the State of *Minas Gerais*, southeastern Brazil, corresponding to an area of about 7,000 km^2. This region is known worldwide for its immense deposits of iron ore, gold, manganese, and several other valuable minerals, which are mined by several industries, from large conglomerates up to countless small-to-medium-sized mining companies.

Dam I constitutes the tailings disposal system from the ore concentration plant of 'Córrego do Feijão', currently owned by Vale S.A. The dam was built using the upstream construction method with a starter dam comprised of fine ore and laterite. The impoundment has been in operation since 1976. Dam I had a maximum height of 81 m with nine raising dykes, built using tailings or compacted soil as construction materials (Fig. 3).

A large-scale investigation was conducted along the main cross-section of the dam (so-called 'reference section'- RS) involving conventional field testing (exploratory borings with standard penetration tests - SPT and cone pen-

Figure 3 - General view of Dam I - 'Córrego do Feijão' Mine.

etration tests - CPT). A total of 12 in situ tests were performed, with four couple SPT - CPT tests in adjacent points, and three SPT tests and one CPT test distributed in different points along the downstream slope of the dam (Fig. 4). In each of them, tailings samples were collected for laboratory tests.

In addition, an extensive laboratory test campaign was also developed in order to complete geotechnical characterization of the tailings, foundation materials and tailings impoundment, that are described and presented elsewhere (Pirete, 2010). The ore tailings from 'Córrego de Feijão' mine (CF tailings) generally consist of uniform fine silty sand (Fig. 5) containing about of 4% clay, 28% of silt,
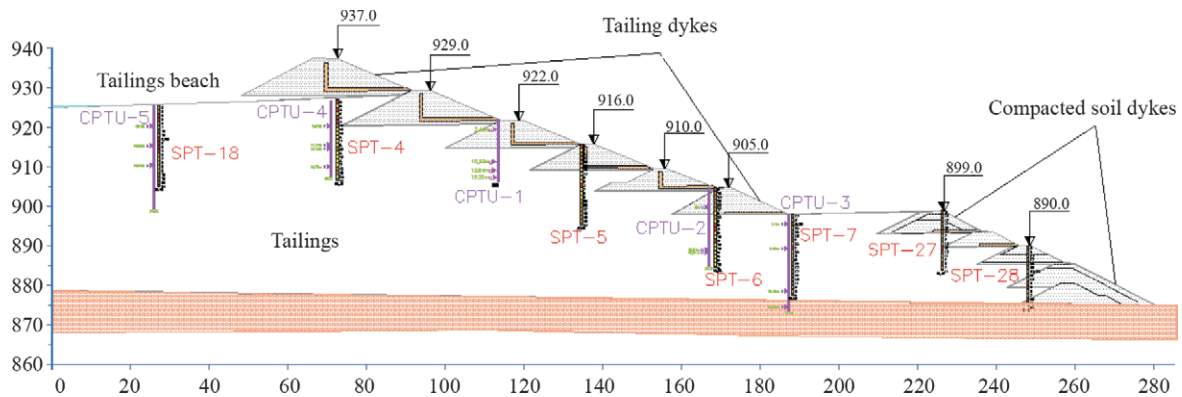
Figure 4 - Typical cross-section of the dam (RS section) and SPT and CPT locations.
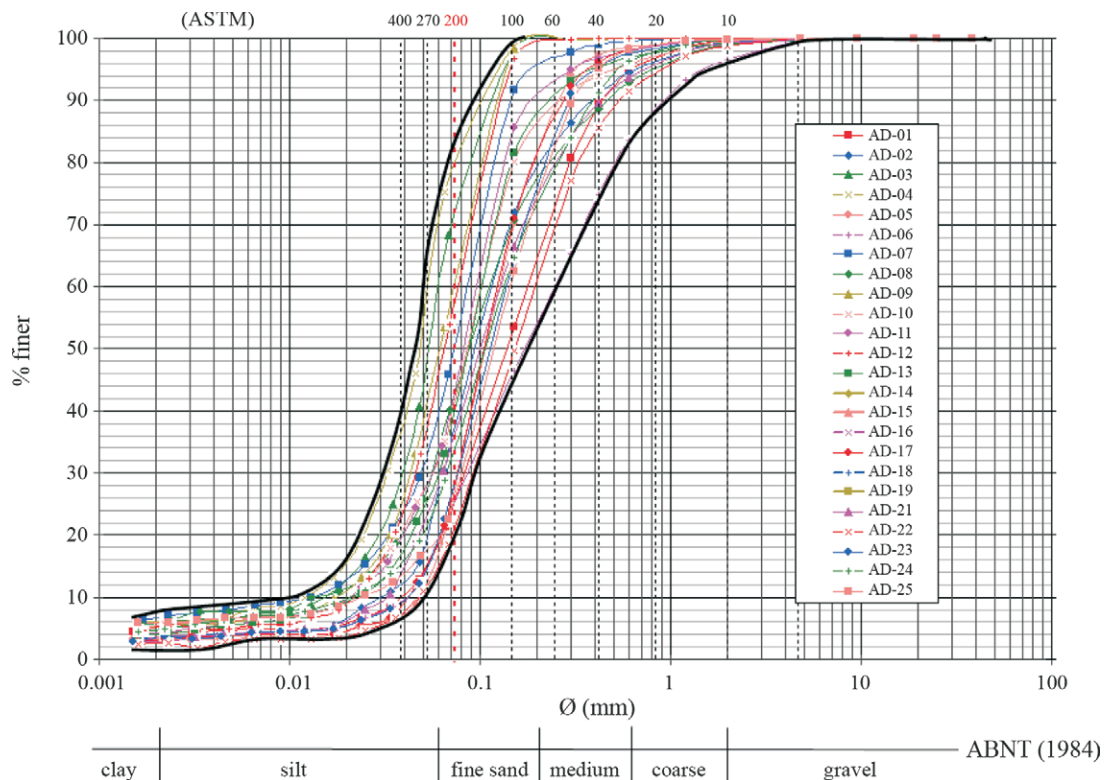
Figure 5 - Particle size distribution curves of CF tailings (ABNT, 1984).

Soils and Rocks, São Paulo, 36(1): 37-53, January-April, 2013.

41

56% of fine sand, 8% of medium sand, 3% of coarse sand and also 1% of gravel (ABNT, 1984). On the other hand, some strata tend to exhibit low plasticity (w$_L$ ≤ 35%) with potential susceptibility to liquefaction mechanisms. The measured maximum void ratio was 1.47 and the minimum void ratio was 0.74. In tailings deposit, values of relative density index varied between 49% and 72%.

4. Liquefaction Analysis of CF Tailings Using Strength Ratios

4.1. CF tailings liquefaction susceptibility

As exposed previously, the first step in evaluating the potential for CF tailings liquefaction is to verify whether these residues are susceptible to undrained strain-softening behavior and flow failure (contractive or dilative behavior) by means of a susceptibility analysis using corrected SPT blowcount values or corrected CPT resistance tip values.

The measured SPT blowcount (N) is normalized for an energy level equal to 60% of the theoretical free-fall hammer energy applied to the drill system (N$_{60}$, where ER is a called 'energy ratio') and for the overburden stress at the depth of the test (multiplying N$_{60}$ by the overburden correction factor C_N ≤ 2.0). The measured SPT blowcount is then corrected to a standardized value of (N$_1$)$_{60}$ as (Olson, 2001):

$$(N_1)_{60} = N\left(\frac{ER}{60}\right)\left(\frac{p_a}{\sigma'_{v0}}\right)^n = N\left(\frac{70}{60}\right)C_N \qquad (1)$$

where σ'_{v0} is the vertical effective stress at the depth of N and p_a is one atmosphere of pressure (approximately 100 kPa) in the same units as σ'_{v0}. The maximum value of 2.0 limits C_N at depths typically less than 1.5 m. The energy ratio ER should be measured for the particular SPT equipment used (70% in this study). Table 1 presents the corrected values for (N$_1$)$_{60}$ along the reference section of Dam I (CF - RS) for SPT-18, SPT-04, SPT-05, SPT-06 tests. Table 2 presents these factors for SPT-07, SPT-27 e SPT-28 tests.

The pairs of values (N$_1$)$_{60}$ and σ'_{v0}, calculated in Tables 3 and 4, were then correlated with the results of back-analysis of historical cases and with the Fear & Robertson (1995) boundary (Fig. 6), delineating field conditions susceptible and not susceptible to flow failure.

In the present analysis, CPT test results are also available, a fact that allows the review of susceptibility to liquefaction of CF - RS tailings based on corrected values of tip resistances, reevaluating the previous approach. However, unlike SPT tests, CPT tests include continuous records of the tailings deposit profile and then tip resistances values (q_c) only need to be corrected for vertical effective stress (q_{c1}).

The measured CPT tip resistance is then corrected to a standardized value of (q_{c1}) and is obtained as follows:
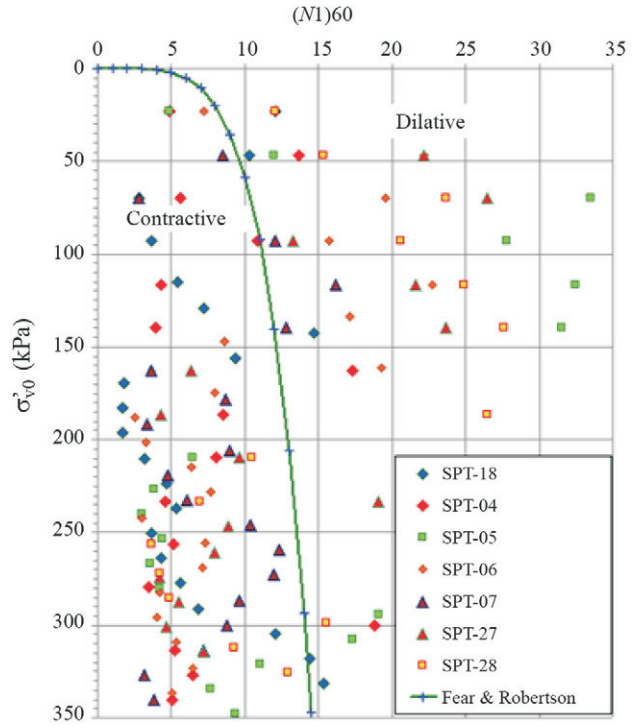
Figure 6 - Relationship (N$_1$)$_{60}$ *versus* σ'_{v0} for CF-RS tailings.

$$q_{c1} = C_q \cdot q_c = \frac{1.8}{0.8 + \left(\sigma'_{v0}/p_a\right)} \cdot q_c \qquad (2)$$

where σ'_{v0} is the vertical effective stress at the depth of (q_c) and p_a is one atmosphere of pressure (approximately 100 kPa) in the same units as σ'_{v0}. The factor C_q should be less or equal to 2.0 (Olson, 2001).

Table 3 presents the corrected values for (q_{c1}) along the reference section of Dam I from 'Córrego do Feijão' mine (CF - RS) for CPT-05, CPT-04 and CPT-01 tests and Table 4 presents these factors for CPT-027 and CPT-03 tests.

Similarly, the pairs of values (q_{c1}) and σ'_{v0}, calculated in Tables 3 and 4, were correlated with the results of back-analysis of historical cases and with the Fear - Robertson (1995) boundary (Fig. 7), delineating tailings susceptible and not susceptible to flow failure.

The results, in both the analysis of SPT and CPT analyses, demonstrate that the most points scored is located to the left of the Fear & Robertson boundary, corresponding to materials that tend to exhibit contractile behavior during shear, i.e., CF tailings liquefaction susceptibility is likely and this analysis should be complemented by the triggering analysis and post-triggering - flow failure stability analysis. For a better characterization of the tailings sub-layers susceptible to liquefaction, based on the SPT and CPT profiles, the authors of this paper developed a technique for further

Table 1 - Standardized values of $(N_1)_{60}$ for SPT-18, SPT-04, SPT-05, SPT-06 tests.

Depth (m)	SPT - 18					SPT - 04					SPT - 05					SPT - 06				
	N	N_{60}	σ'_{vo} (kPa)	WT CN	4.90m $(N_1)_{60}$	N	N_{60}	σ'_{vo} (kPa)	WT CN	12.72m $(N_1)_{60}$	N	N_{60}	σ'_{vo} (kPa)	WT CN	9.33m $(N_1)_{60}$	N	N_{60}	σ'_{vo} (kPa)	WT CN	5.40m $(N_1)_{60}$
1	5	5.83	23.30	2.07	12.1	2	2.33	23.30	2.07	4.8	2	2.33	23.30	2.07	4.83	3	3.50	23.30	2.07	7.25
2	6	7.00	46.60	1.46	10.3	8	9.33	46.60	1.46	13.7	7	8.17	46.60	1.46	11.96	13	15.17	46.60	1.46	22.22
3	2	2.33	69.90	1.20	2.8	4	4.67	69.90	1.20	5.6	24	28.00	69.90	1.20	33.49	14	16.33	69.90	1.20	19.54
4	3	3.50	93.20	1.04	3.6	9	10.50	93.20	1.04	10.9	23	26.83	93.20	1.04	27.79	13	15.17	93.20	1.04	15.71
5	5	5.83	115.52	0.93	5.4	4	4.67	116.50	0.93	4.3	30	35.00	116.50	0.93	32.43	21	24.50	116.50	0.93	22.70
6	7	8.17	129.02	0.88	7.2	4	4.67	139.80	0.85	3.9	32	37.33	139.80	0.85	31.57	17	19.83	133.92	0.86	17.14
7	15	17.50	142.52	0.84	14.7	19	22.17	163.10	0.78	17.4	39	45.50	163.10	0.78	35.63	9	10.50	147.42	0.82	8.65
8	10	11.67	156.02	0.80	9.3	10	11.67	186.40	0.73	8.5	44	51.33	186.40	0.73	37.60	21	24.50	160.92	0.79	19.31
9	2	2.33	169.52	0.77	1.8	10	11.67	209.70	0.69	8.1	8	9.33	209.70	0.69	6.45	9	10.50	174.42	0.76	7.95
10	2	2.33	183.02	0.74	1.7	6	7.00	233.00	0.66	4.6	5	5.83	226.43	0.66	3.88	3	3.50	187.92	0.73	2.55
11	2	2.33	196.52	0.71	1.7	7	8.17	256.30	0.62	5.1	4	4.67	239.93	0.65	3.01	4	4.67	201.42	0.70	3.29
12	4	4.67	210.02	0.69	3.2	5	5.83	279.60	0.60	3.5	6	7.00	253.43	0.63	4.40	8	9.33	214.92	0.68	6.37
13	6	7.00	223.52	0.67	4.7	28	32.67	300.16	0.58	18.9	5	5.83	266.93	0.61	3.57	10	11.67	228.42	0.66	7.72
14	7	8.17	237.02	0.65	5.3	8	9.33	313.66	0.56	5.3	6	7.00	280.43	0.60	4.18	4	4.67	241.92	0.64	3.00
15	5	5.83	250.52	0.63	3.7	10	11.67	327.16	0.55	6.5	28	32.67	293.93	0.58	19.1	10	11.67	255.42	0.63	7.30
16	6	7.00	264.02	0.62	4.3	8	9.33	340.66	0.54	5.1	26	30.33	307.43	0.57	17.3	10	11.67	268.92	0.61	7.11
17	8	9.33	277.52	0.60	5.6	7	8.17	354.16	0.53	4.3	17	19.83	320.93	0.56	11.07	6	7.00	282.42	0.60	4.17
18	10	11.67	291.02	0.59	6.8	13	15.17	367.66	0.52	7.9	12	14.00	334.43	0.55	7.66	6	7.00	295.92	0.58	4.07
19	18	21.00	304.52	0.57	12.0	15	17.50	381.16	0.51	9.0	15	17.50	347.93	0.54	9.38	8	9.33	309.42	0.57	5.31
20	22	25.67	318.02	0.56	14.4	34	39.67	394.66	0.50	20.0	16	18.67	361.43	0.53	9.82	10	11.67	322.92	0.56	6.49
21	24	28.00	331.52	0.55	15.4	21	24.50	408.16	0.49	12.1	13	15.17	374.93	0.52	7.83	8	9.33	336.42	0.55	5.09

Table 2 - Standardized values of $(N_1)_{60}$ for SPT-07, SPT-27 e SPT-28 tests.

depth. (m)	SPT - 07					SPT - 27					SPT - 28			
	N	N_{60}	σ'_{vo} (KPa)	WT CN	7.20m $(N_1)_{60}$	N	N_{60}	σ'_{vo} (KPa)	WT CN	10.05m $(N_1)_{60}$	N	N_{60}	σ'_{vo} (KPa)	WT CN
1	17	19.83	23.30	2.07	41.09	21	24.50	23.30	2.07	50.76	5	5.83	23.30	2.07
2	5	5.83	46.60	1.46	8.55	13	15.17	46.60	1.46	22.22	9	10.50	46.60	1.46
3	2	2.33	69.90	1.20	2.79	19	22.17	69.90	1.20	26.51	17	19.83	69.90	1.20
4	10	11.67	93.20	1.04	12.08	11	12.83	93.20	1.04	13.29	17	19.83	93.20	1.04
5	15	17.50	116.50	0.93	16.21	20	23.33	116.50	0.93	21.62	23	26.83	116.50	0.93
6	13	15.17	139.80	0.85	12.8	24	28.00	139.80	0.85	23.68	28	32.67	139.80	0.85
7	4	4.67	163.10	0.78	3.65	7	8.17	163.10	0.78	6.39	45	52.50	163.10	0.78
8	10	11.67	178.56	0.75	8.73	5	5.83	186.40	0.73	4.27	31	36.17	186.40	0.73
9	4	4.67	192.06	0.72	3.37	12	14.00	209.70	0.69	9.67	13	15.17	209.70	0.69
10	11	12.83	205.56	0.70	8.95	25	29.17	233.00	0.66	19.1	9	10.50	233.00	0.66
11	6	7.00	219.06	0.68	4.73	12	14.00	246.99	0.64	8.91	5	5.83	256.30	0.62
12	8	9.33	232.56	0.66	6.12	11	12.83	260.49	0.62	7.95	6	7.00	271.76	0.61
13	14	16.33	246.06	0.64	10.4	6	7.00	273.99	0.60	4.23	7	8.17	285.26	0.59
14	17	19.83	259.56	0.62	12.3	8	9.33	287.49	0.59	5.50	23	26.83	298.76	0.58
15	17	19.83	273.06	0.61	12.00	7	8.17	300.99	0.58	4.71	14	16.33	312.26	0.57
16	14	16.33	286.56	0.59	9.65	11	12.83	314.49	0.56	7.24	20	23.33	325.76	0.55
17	13	15.17	300.06	0.58	8.76			327.99					339.26	
18	11	12.83	313.56	0.56	7.25			341.49					352.76	
19	5	5.83	327.06	0.55	3.23			354.99					366.26	
20	6	7.00	340.56	0.54	3.79			368.49					379.76	
21	4	4.67	354.06	0.53	2.48			381.99					393.26	

refinement of the data, according to the procedures described below.

4.2. CF-SR profile divided in tailings sub-layers susceptible to liquefaction

Initially, the values of the parameters $(N_1)_{60}$ were correlated with their respective elevations, in order to characterize the critical zones of potential liquefaction-induced flow along the tailings deposit, considering the domain limited by values of $(N_1)_{60} \leq 12$ (Eq. 5). The regions with average values of $(N_1)_{60} \leq 6$ were classified as zones of low resistance whereas the regions with average values of $6 < (N_1)_{60} \leq 12$ were classified as zones of medium resistance (Fig. 8).

This subdivision was extrapolated then for the CF - RS profile of the downstream slope of Dam I, resulting in nine layers susceptible to liquefaction (Fig. 9), with resistances given by the mean values obtained from the correspondent SPT profile zones.

Additionally, the values of the respective parameters (q_{c1}) were correlated with their elevations, in order to characterize the critical zones of potential liquefaction-induced

flow along the tailings deposit, considering the domain limited by values of $(q_{c1}) \leq 6.5$ MPa (Eq. 6). The regions with average values of $(N_1)_{60} \leq 3.25$ MPa were classified as zones of low resistance whereas the regions with average values of 3.25 MPa $< (N_1)_{60} \leq 6.5$ MPa were classified as zones of medium resistance (Fig. 10).

This subdivision was extrapolated similarly to the CF - RS profile of the downstream slope of Dam I, resulting also in nine layers susceptible to liquefaction (Fig. 11), including SPT - 05 results for better characterization, with resistances given by the mean values obtained from the correspondent CPT profile zones.

The comparison between Figs. 9 and 11 indicates a good correlation of both geometries of the tailings deposit, with the characterization of nine layers that have a greater potential or susceptibility to liquefaction. The largest differences occurred for layers located near the edge of the intermediate dykes (layers 06, 07 and 08), both in terms of thickness and mean values of resistance. Based on this refined set of layers to the CF - RS profile of the downstream slope, the triggering analysis was then applied to the ore tailings deposited in Dam I from 'Córrego do Feijão' mine.

44

Soils and Rocks, São Paulo, 36(1): 37-53, January-April, 2013.

Table 3 - Standardized values of (q_{c1}) for CPT-05, CPT-04 and CPT-01 tests.

depth (m)	CPT - 05					CPT - 04					CPT - 01				
	q_c (MPa)	σ'_{vo} (MPa)	σ'_{vo} (KPa)	WT Cq	4.90m q_{c1} (MPa)	q_c (MPa)	σ'_{vo} (MPa)	σ'_{vo} (KPa)	WT Cq	12.72m q_{c1} (MPa)	q_c (MPa)	σ'_{vo} (MPa)	σ'_{vo} (KPa)	WT Cq	13.20m q_{c1} (MPa)
1	1.903	0.02	23.30	1.74	3.32	3.48	0.023	23.30	1.74	6.1					
2	1.289	0.05	46.60	1.42	1.83	3.726	0.047	46.60	1.42	5.3	31.099	0.047	46.60	1.42	44.2
3	0.965	0.07	69.90	1.20	1.16	2.736	0.070	69.90	1.20	3.3	38.779	0.070	69.90	1.20	46.6
4	1.735	0.09	93.20	1.04	1.80	3.44	0.093	93.20	1.04	3.6	28.29	0.093	93.20	1.04	29.4
5	1.003	0.12	115.52	0.92	0.92	2.521	0.117	116.50	0.92	2.3	24.152	0.117	116.50	0.92	22.1
6	0.264	0.13	129.02	0.86	0.23	2.776	0.140	139.80	0.82	2.3	48.328	0.140	139.80	0.82	39.6
7	7.734	0.14	142.52	0.81	6.26	21.171	0.163	163.10	0.74	15.7	52.6	0.163	163.10	0.74	38.9
8	3.739	0.16	156.02	0.76	2.85	8.916	0.186	186.40	0.68	6.0	15.6	0.186	186.40	0.68	10.5
9	3.379	0.17	169.52	0.72	2.44	7.389	0.210	209.70	0.62	4.6	9.6	0.210	209.70	0.62	6.00
10	0.819	0.18	183.02	0.68	0.56	3.61	0.233	233.00	0.58	2.1	5.325	0.233	233.00	0.58	3.10
11	0.508	0.20	196.52	0.65	0.33	5.127	0.256	256.30	0.54	2.74	9.663	0.256	256.30	0.54	5.17
12	0.574	0.21	210.02	0.62	0.36	1.001	0.280	279.60	0.50	0.50	8.178	0.280	279.60	0.50	4.09
13	3.926	0.22	223.52	0.59	2.33	8.508	0.300	300.16	0.47	4.03	2.757	0.303	302.90	0.47	1.30
14	8.01	0.24	237.02	0.57	4.55	10.016	0.314	313.66	0.46	4.58	1.733	0.318	318.36	0.45	0.78
15	0.857	0.25	250.52	0.54	0.47	7.009	0.327	327.16	0.44	3.10	19.098	0.332	331.86	0.44	8.35
16	0.984	0.26	264.02	0.52	0.51	7.059	0.341	340.66	0.43	3.02	23.652	0.345	345.36	0.42	10.01
17	7.301	0.28	277.52	0.50	3.68	1.277	0.354	354.16	0.41	0.53					
18	16.419	0.29	291.02	0.49	7.97	4.455	0.368	367.66	0.40	1.79					
19	14.846	0.30	304.52	0.47	6.95	8.562	0.381	381.16	0.39	3.34					
20	14.997	0.32	318.02	0.45	6.78	26.112	0.395	394.66	0.38	9.90					
21	10.706	0.33	331.52	0.44	4.68										

Table 4 - Standardized values of (q_{c1}) for CPT-027 and CPT-03 tests.

| depth. (m)	CPT - 02					CPT - 03				
	q_c (MPa)	σ'_{vo} (MPa)	σ'_{vo} (kPa)	WT Cq	5.40m q_{c1} (MPa)	q_c (MPa)	σ'_{vo} (MPa)	σ'_{vo} (kPa)	WT Cq	7.20m q_{c1} (MPa)
1	21.039	0.023	23.30	1.74	36.66	12.533	0.023	23.30	1.74	21.84
2	16.475	0.047	46.60	1.42	23.42	4.598	0.047	46.60	1.42	6.54
3	24.461	0.070	69.90	1.20	29.37	1.003	0.070	69.90	1.20	1.20
4	35.824	0.093	93.20	1.04	37.23	5.757	0.093	93.20	1.04	5.98
5	31.5	0.117	116.50	0.92	28.85	11.15	0.117	116.50	0.92	10.21
6	6.178	0.134	133.92	0.84	5.20	6.364	0.140	139.80	0.82	5.21
7	3.414	0.147	147.42	0.79	2.70	4.842	0.163	163.10	0.74	3.59
8	31.26	0.161	160.92	0.75	23.36	6.292	0.179	178.56	0.70	4.38
9	9.606	0.174	174.42	0.71	6.80	1.883	0.192	192.06	0.66	1.25
10	7.252	0.188	187.92	0.67	4.87	13.189	0.206	205.56	0.63	8.31
11	7.4	0.201	201.42	0.64	4.73	8.51	0.219	219.06	0.60	5.12
12	8.177	0.215	214.92	0.61	4.99	4.365	0.233	232.56	0.58	2.51
13	6.8	0.228	228.42	0.58	3.97	11.379	0.246	246.06	0.55	6.28
14	3.9	0.242	241.92	0.56	2.18	15.821	0.260	259.56	0.53	8.39
15	4.6	0.255	255.42	0.54	2.47	4.513	0.273	273.06	0.51	2.30
16	2.832	0.269	268.92	0.52	1.46	16.437	0.287	286.56	0.49	8.07
17	9.733	0.282	282.42	0.50	4.83	10.536	0.300	300.06	0.47	4.99
18	11.627	0.296	295.92	0.48	5.57	7.759	0.314	313.56	0.46	3.55
19	11.56	0.309	309.42	0.46	5.34	5.411	0.327	327.06	0.44	2.39
20	8.869	0.323	322.92	0.45	3.96	1.648	0.341	340.56	0.43	0.71
21						1.204	0.354	354.06	0.41	0.50
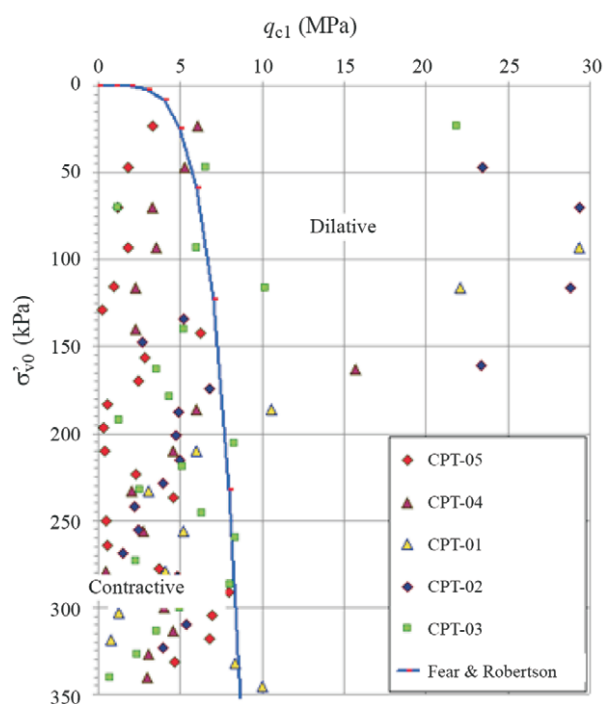
**Figure 7** - Relationship (q_{c1}) *versus* σ'_{v0} for CF-RS tailings.

4.3. CF Tailings liquefaction triggering analysis

The methodology adopted for the triggering analysis included the following procedures (Olson and Stark, 2003b):

i From the liquefaction geometry of the reference section of the dam obtained from SPT test results (Fig. 9), limit equilibrium stability analyses were implemented using the method of Spencer (1967) and considering non-circular and circular surfaces (software Slide 5.043 from Rocscience International). Different values of shear strength were assumed for the soil layers susceptible to liquefaction, varying this resistance continually until obtaining FS = 1.0 and the corresponding critical surface rupture, defined for a critical value $\tau_d = 45$ kPa (indicated in Fig. 9). The critical failure surface obtained in the analysis tends to extend from the seventh rising to the horizontal platform located between the third and fourth dykes (a 60 m displacement of the fourth dyke axle towards upstream was performed to improve general stability of the dam), crossing the layers 5 and 6 of the tailings sus-

46

Soils and Rocks, São Paulo, 36(1): 37-53, January-April, 2013.
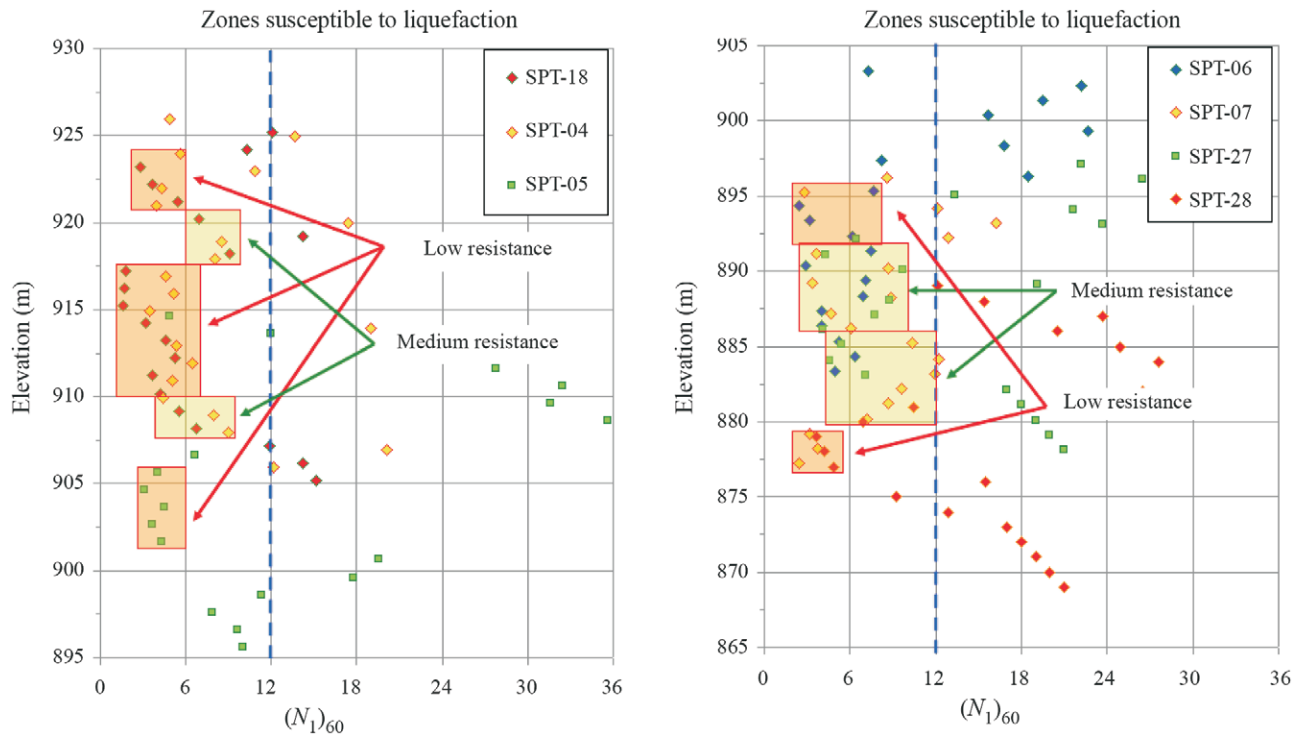
Figure 8 - RS - SPT profile divided in layers susceptible to liquefaction for $(N_1)_{60} \leq 12$.
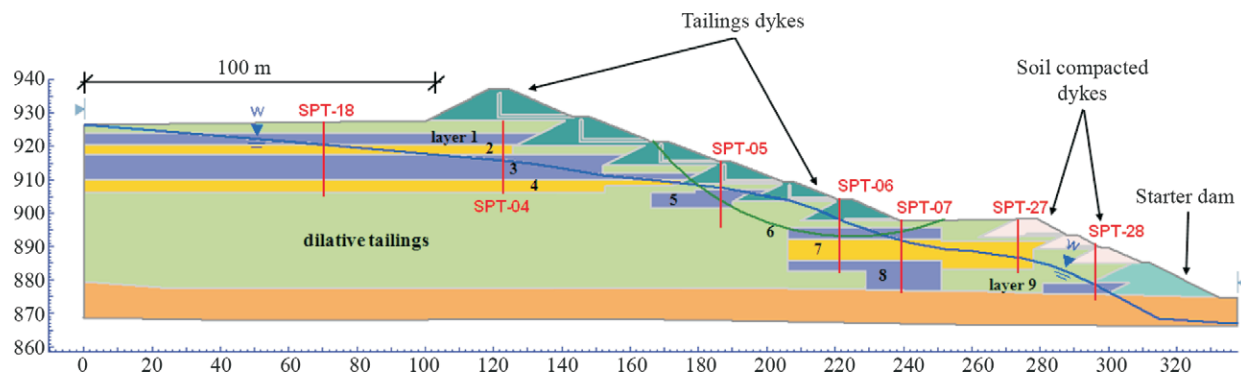
Figure 9 - CF - RS subdivided in nine layers susceptible to liquefaction (SPT analysis).

ceptible to liquefaction and that should therefore be subject to corresponding triggering analysis.

ii   Division of the yield failure surface into 16 segments (Fig. 12)

iii   From the determination of the weighted effective vertical stress, σ'_{v0} (Eq. 3), along the critical failure surface (within the domain of tailings susceptible to liquefaction), the average static shear stress ratio τ_d / σ'_{v0} (average value) was equal to 45 kPa / 217 kPa → 0.207.

iv   Average seismic shear stress is not applicable in this case and then $(\tau_{sism})_{avg} = 0$.

v   Table 5 presents the yield strength ratio values $(s_{u(yield)}/\sigma'_{v0})$ for layers 5 and 6 based on corrected SPT results.

The ratio values were used to obtain $S_{u(yield)}$ and τ_d for each segment based on respective σ'_{v0} values. For static loadings (Eq. 7), in this critical zone, the $(FS)_{triggering}$ is generally greater than 1.1 (typically varying between 1.14 and 1.21 as indicated in Table 6), indicating that CF - SR tailings are unlikely to liquefy.

Adopting the same methodology for the CPT results, the location of the critical surface rupture (for $\tau_d = 45$ kPa)

Table 5 - Yield strength ratio values $(s_{u(yield)}/\sigma'_{v0})$ for layers 5 and 6 (SPT analysis).

| Layers	$(N_1)_{60}$	$s_{u(yield)}/\sigma'_{v0}$
05	4.5	0.239
06	6.0	0.250

**Table 6** - Liquefaction triggering results for CF - RS tailings (SPT analysis).

Segment N°	Liquefiable?	σ'_{vo} (kPa)	$(\tau_d)/\sigma'_{vo\ (average)}$	$s_u(yield)/\sigma'_{vo}$	s_u (yield)	$\tau_{driving}$ (τ_d)	$FS_{Triggering}$	Liquefaction triggered?
1	No	-	-	-	-	-	-	-
2	No	-	-	-	-	-	-	-
3	Yes	140.48	0.21	0.241	33.86	29.50	1.15	No
4	No	-	-	-	-	-		-
5	No	-	-	-	-	-		-
6	Yes	187.38	0.21	0.239	44.78	39.35	1.14	No
7	No	-	-	-	-	-	-	-
8	No	-	-	-	-	-	-	-
9	No	-	-	-	-	-	-	-
10	Yes	232.12	0.21	0.250	58.03	48.75	1.19	No
11	Yes	232.03	0.21	0.250	58.01	48.73	1.19	No
12	Yes	235.92	0.21	0.250	58.98	49.54	1.19	No
13	Yes	218.95	0.21	0.250	54.74	45.98	1.19	No
14	Yes	155.14	0.21	0.250	38.79	32.58	1.19	No
15	Yes	80.71	0.21	0.250	20.18	16.95	1.19	No
16	No	-	-	-	-	-	-	-

along the downstream slope of the tailings dam is indicated in Fig. 11 (crossing the layers 5 and 6 of the tailings susceptible to liquefaction), essentially similar to the previous critical surface (based on SPT results).

Considering its division into 16 segments and applying the steps (iii), (iv) and (v) from the methodology, were obtained the yield strength ratio values ($s_{u(yield)}/\sigma'_{v0}$) for layers 5 and 6 indicated in Table 7.
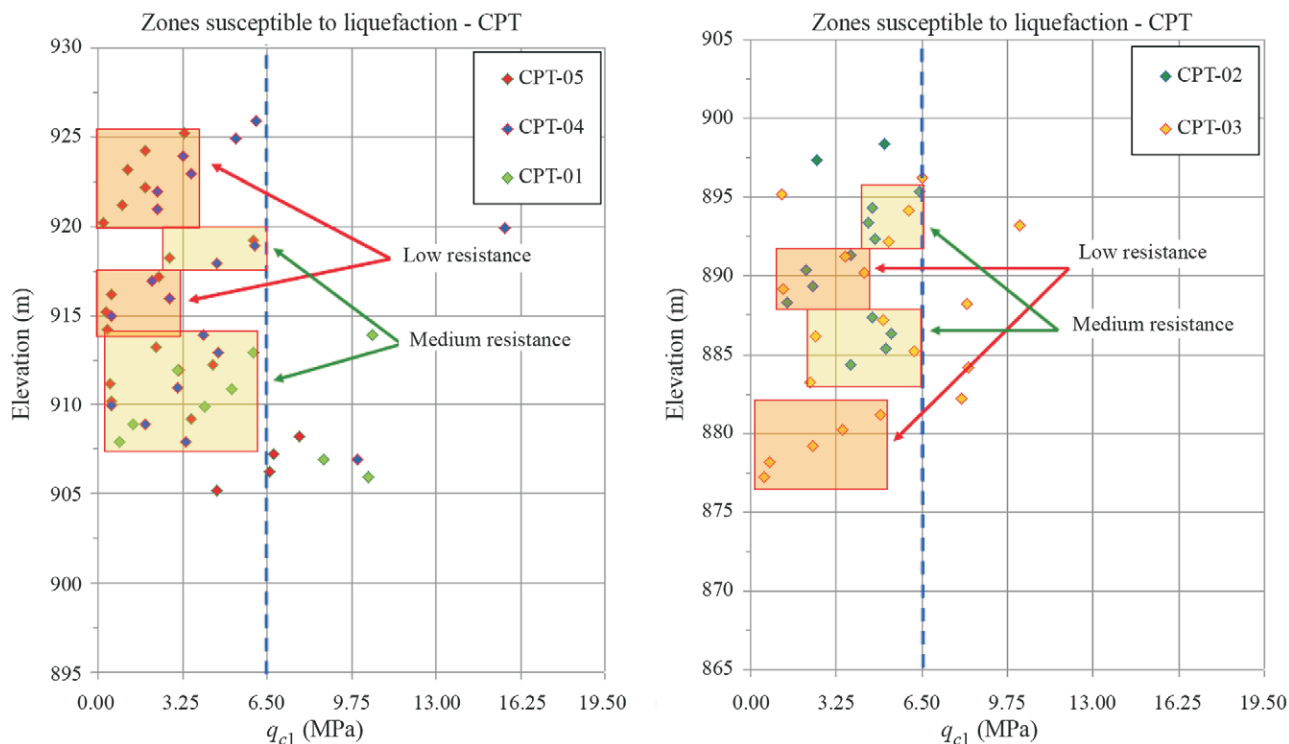
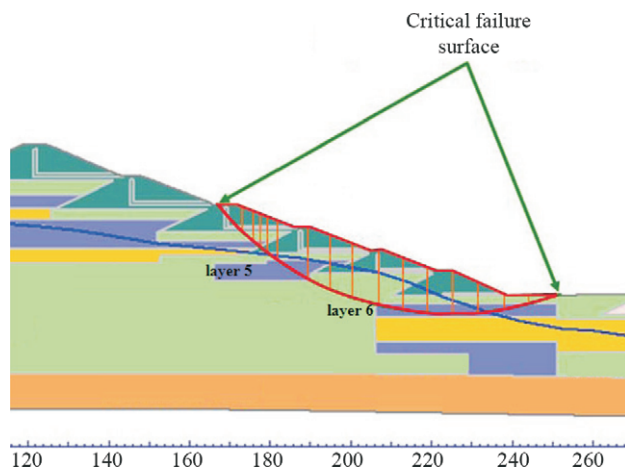**Figure 10** - RS - CPT profile divided in layers susceptible to liquefaction for (q_{c1}) $\leq$ 6.5 Mpa.
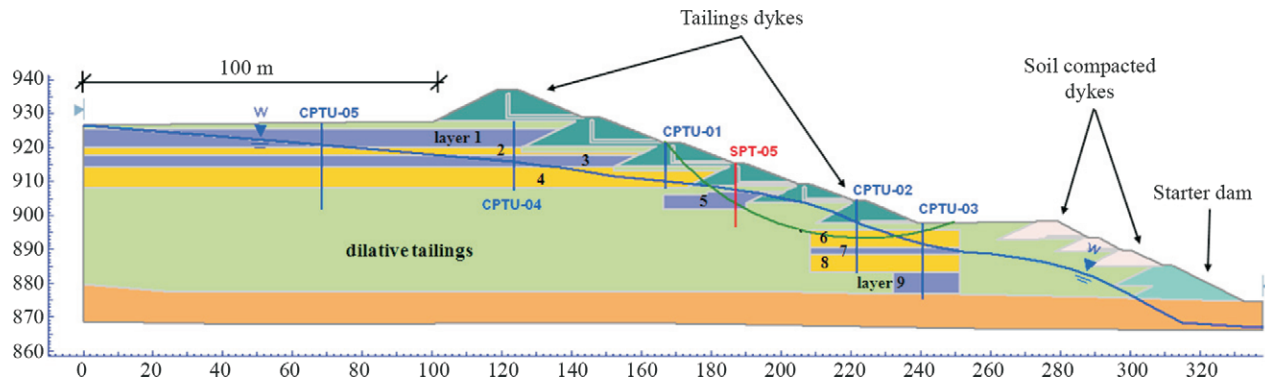
Figure 11 - CF - RS subdivided in nine layers susceptible to liquefaction (CPT analysis).

Table 7 - Yield strength ratio values ($s_{u(yield)}/\sigma'_{v0}$) for layers 5 and 6 (CPT analysis).

Layers	(q_{c1})	$s_{u(yield)}/\sigma'_{v0}$
05	4 5*	0.239
06	5.4 MPa	0.282

* $(N_1)_{60}$ parameter.

Figure 12 - Yield failure surface divided into 16 segments.

Once more, in the hypothesis of only static loading, the $(FS)_{triggering}$ is generally greater than 1.1 (typically varying between 1.15 and 1.36 as indicated in Table 8), indicating that CF - SR tailings are unlikely to liquefy.

4.4. CF Tailings liquefaction post-triggering analysis

In both triggering liquefaction analyses, using the results of SPT and CPT tests performed in the reference section of the Dam I, all segments from tailings critical zones have $(FS)_{triggering} > 1.0$ and then post-triggering stability analysis is unnecessary to verify whether the static shear forces exceed the available shear resistance (including liquefied shear strength). Nevertheless, a post-triggering slope stability analysis was appropriate since it was conducted using

appropriate yield shear strength values instead of liquefied shear strength values.

Table 9 presents the geotechnical parameters used in stability analyses of the downstream slope. These parameters were obtained from a series of undrained triaxial compression tests performed under monotonic loading conditions on reconstituted samples of the tailings. All the specimens were isotropically consolidated at a mean effective pressure of 100 kPa, 200 kPa, 300 kPa and 400 kPa and then, subjected to undrained monotonic loading at a constant strain rate of 0.09 mm per minute, which was slow enough to allow the pore pressure change to equalize throughout the sample with pore pres-sure measured at the base of sample. All tests were con-tinued up to a 20% axial strain. The yield strength ratio values were taken from SPT results.

Phreatic surface location is one of the most important factors to influence tailings dam safety, under both static and seismic loading conditions (Vick, 1990). The major design premise is that the phreatic surface should not emerge from the embankment and should be as low as possible near the embankment face. Thus, any factors that might affect the phreatic surface affect directly the dam stability and can be caused by any changes in environmental or operating conditions (heavy rainfall, blockage of seepage outlets, rise in water levels of the pond, etc.)

For the post-triggering analysis, a rapid rise of the phreatic line was admitted through the tailings deposit emerging from the embankment and reaching the toes of the intermediate rising dykes, with complete saturation of tailings layers susceptible to liquefaction. The initial position of the phreatic line was given from readings given by dam piezometers and by a 100 m extension of the tailings beach. Figures 13 and 14 present the results of the stability analyses for a strong rise of the phreatic line in Dam I based on SPT and CPT configurations, respectively.

The results are closely similar in terms of the critical failure surface location and of the safety factor values against flow failure $(FS)_{flow}$ for SPT and CPT configurations (1.28 and 1.32, respectively). These values imply that the flow failure susceptibility of Dam I is low even under such

Table 8 - Liquefaction triggering results for CF - RS tailings (CPT analysis).

Segment N°	Liquefiable?	σ'_{vo} (kPa)	$(\tau_d)/\sigma'_{vo\ (average)}$	$s_u(yield)/\sigma'_{vo}$	s_u (yield)	$\tau_{driving}$ (τ_d)	$FS_{Triggering}$	Liquefaction triggered?
1	No	-	-	-	-	-	-	-
2	No	-	-	-	-	-	-	-
3	Yes	135 46	0 21	0 259	35 08	28 45	1 23	No
4	No	-	-	-	-	-	-	-
5	No	-	-	-	-	-	-	-
6	Yes	187 09	0 21	0 239	44 71	39 29	1 14	No
7	No	-	-	-	-	-	-	-
8	No	-	-	-	-	-	-	-
9	No	-	-	-	-	-	-	-
10	Yes	233 96	0 21	0 282	65 98	49 13	1 34	No
11	Yes	230 39	0 21	0 282	64 97	48 38	1 34	No
12	Yes	236 07	0 21	0 282	66 57	49 57	1 34	No
13	Yes	216 30	0 21	0 282	61 00	45 42	1 34	No
14	Yes	160 22	0 21	0 282	45 18	33 65	1 34	No
15	Yes	79 24	0 21	0 282	22 35	16 64	1 34	No
16	No	-	-	-	-	-	-	-

Table 9 - Geotechnical parameters for the post-triggering downstream slope stability analyses.

Material	y (kN/m^3)	C (kPa)	ø (°)	s_u (yield)/σ'_{vo}
Residual soil (foundation)	20	20	30	-
Starter dam (compacted soil)	20	5	36	-
Compacted soil	20	10	30	-
Compacted tailings	25	5	40	-
Dilative tailings	22	20	38	-
Layer 1	22	-	-	0.238
Layer 2	22	-	-	0.267
Layer 3 and 5	22	-	-	0.239
Layer 4	22	-	-	0.255
Layer 6 8 and 9	22	-	-	0.250
Layer 7	22	-	-	0.260

a critical loading event, based on the following proposed range to evaluate flow failure potential in these analyses:

- $(FS)_{flow}$ 3 1.5: → Unlike;
- $1.3 \leq (FS)_{flow} < 1.5$: → Low;
- $1.1 \leq (FS)_{flow} < 1.3$: → Moderate;
- $(FS)_{flow} < 1.1$: → High.

An extensive laboratory experimental program has been performed, including strain-controlled, undrained-triaxial tests to measure: (i) the peak undrained strength, (ii) the shear strain to peak undrained strength, and (iii) the drop-off in shearing resistance with continued strain after peak. Test specimens were con-solidated isotropically and anisotropically to stresses aiming to model in situ conditions. Based on these laboratory parameters, new stability analyses were performed and showed in good agreement with the results from the strength ratio analyses presented in this paper.

In addition, the management of the Dam I from 'Córrego do Feijão' has included a rigid water level control using both proper decanting and spigotting procedures to maintain a 100 m minimum distance between the pond's edge and the embankment crest, beyond a continuous program of inspection and maintenance of tailings deposition
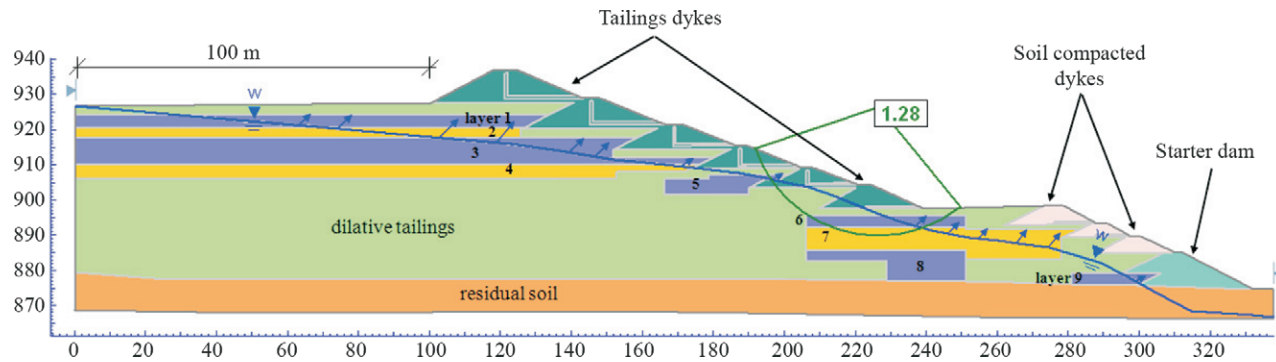
50

Soils and Rocks, São Paulo, 36(1): 37-53, January-April, 2013.

Figure 13 - CF - RS downstream slope: post-triggering stability (SPT analysis).
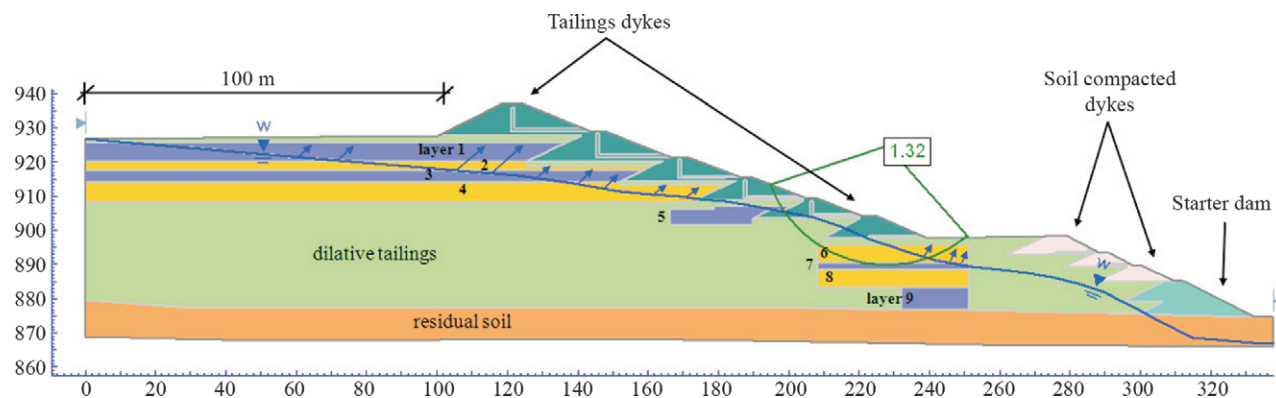
Figure 14 - CF - RS downstream slope: post-triggering stability (CPT analysis).

5. Conclusions

Slope stability analyses involving liquefied soil require that the shear resistance of the softened soil be estimated. In light of the complex nature of excess pore pressure generation, large-strain development, and post-liquefaction strength gain accompanying drainage and large strain, most methods used in practice for estimating the residual strength of liquefied soil rely on back-analysis of field case studies involving slope failures. The most widely used methods based on SPT and CPT results. CPT's tests have the advantage that they are faster to perform and provide a con-tinuous, more reliable profile of penetration resistance.

In this context, Olson (2001) and Olson & Stark (2003b) liquefaction analysis, based on strength ratios approach, is too general, comprising three different approaches: (i) liquefaction susceptibility analysis; (ii) triggering analysis; and (iii) post-triggering - flow failure stability analysis. The method can be used to evaluate whether a specific loading (static or seismic) will produce shear stresses in a zone of a soil that is high enough to cause strength loss in that zone. The basic concept of the method is that strength loss will be triggered by a specific loading event if the sum of the static (gravity) shear stresses along a potential failure surface plus the eventual seismic (or other stresses) shear stresses exceed the yield (peak) undrained strength S_u (yield).

This liquefaction analysis procedure was applied to a Dam I from "Córrego do Feijão" mine, an 81 m high ore tailings disposal system (CF tailings), located in the *Quadrilátero Ferrífero* (Iron Quadrangle) region / Brazil, resulting in the following conclusions:

- CF tailings tend to exhibit contractile behavior during shear and then these materials are susceptible to liquefaction;

- The referenced subdivided section of the downstream slope of Dam I resulted in nine layers being susceptible to liquefaction with resistances given by the mean values obtained from both SPT or CPT profile zones;

- From the specific critical failure surfaces along the downstream slope of Dam I (obtained from SPT or CPT corrected values and subdivided into 16 segments), was obtained an average static shear stress ratio value (τ_d/σ'_{v0}) equal to 0,207 through the critical domain of tailings susceptible to liquefaction;

- In the hypothesis of only static loading, the $(FS)_{triggering}$ values varied between 1.14 and 1.36, indicating that CF - SR tailings are unlikely to liquefy;

- Considering a rapid rise of the phreatic line through the tailings deposit reaching the toes of the intermediate rising dykes, with complete saturation of tailings layers susceptible to liquefied, a post-triggering analysis indicated that the flow failure susceptibility of the Dam I is low even under a such critical loading event;

- The conclusions of these analyses, in addition to laboratory testing program results and based on rigid management procedures adopted in field, demonstrate that Dam I constitutes a safety structure against mechanisms from liquefaction-induced failures;

- Although the Olson (2001) and Olson & Stark (2003b) liquefaction analysis has been proposed mainly for cohesionless soils, the methodology is consistent and suitable for preliminary analyses of liquefaction potential in tailings deposits (generally relatively low- density materials with a high degree of saturation), particularly upstream tailings dams.

References

ABNT - NBR 7181 (1984) Solo - Análise Granulométrica (Grain Size Distribution). Brazilian Association of Technical Standards, Rio de Janeiro.

Aubertin, M.; Mbonimpa, M.; Bussiere, B. & Chapuis, R.P. (2003) A model to predict the water retention curve from basic geotechnical properties. Canadian Geotechnical Journal, v. 40:6, p. 1104-1102.

Bray, J.D.; Sancio, R.B.; Riemer, M. & Durgunoglu, H.T. (2004) Liquefaction susceptibility of fine-grained soils. Proc. 11th ICSD and 3th ICEGE, UC Berkeley, January 2004, pp. 7-9.

Byrne, P.M. (2008) Parecer Técnico (Technical Report), Mina do Cauê, Alteamento do Cordão Nova Vista, Complexo Minerador de Itabira. VALE, Itabira, Minas Gerais, 10 pp.

Casagrande, A. (1975) Liquefaction and cyclic deformation of sands - A critical review. Proc. 5th Pan-American Conference, Argentina, pp. 81-133.

Castro, G. (1975) Liquefaction and cyclic mobility of saturated sands. Journal of the Geotechnical Engineering Division, ASCE, v. 101:GT6, p. 551-569.

Davies, M.P.; McRoberts, E.C. & Martin, T.E. (2002) Static liquefaction of tailings - Fundamentals and case histories. Proc. Tailings Dams 2002. ASDSO/USCOLD, Las Vegas.

Fear, C.E. & Robertson, P.K. (1995) Estimating the undrained strength of sand: A theoretical framework. Canadian Geotechnical Journal, v. 32:4, p. 859-870.

Gomes, R.C. (2010) Mecânica da Liquefação dos Solos (Mechanics of Soil Liquefaction). NUGEO, Federal University of Ouro Preto, 112 pp.

Gomes, R.C.; Pereira, E.L.; Ribeiro, L.F.M. & Silva, J.T.G. (2002) Evaluation of liquefaction potential of fine grained tailings. Proc. International Congress on Environmental Geotechnics, ICEG, Rio de Janeiro. Swets and Zeitlinger, Netherlands, v. 1, p. 329-333.

ICOLD & UNEP (2001) Bulletin 121: Tailings Dams - Risk of Dangerous Occurrences. Lessons Learnt From Practical Experiences. Paris, ICOLD, 144 pp.

Idriss, I.M. & Boulanger, R.W. (2007) SPT- and CPT-based relationships for the residual shear strength of liquefied soils. Proc. Earthquake Geotechnical Engineering, 4th International Conference on Earthquake Geotechnical Engineering - Invited Lectures. K.D. Pitilakis, ed., Springer, The Netherlands, pp. 1-22.

Ishihara, K. (1993) Liquefaction and flow failure during earthquakes. Geotechnique, v. 43:3, p. 351-415.

Ishihara, K.; Yasuda, S. & Yoshida, Y. (1990) Liquefaction-induced flow failure of embankments and residual strength of silty sands. Soils and Foundations, v. 30:3, p. 69-80.

Kramer, S.L. (1996) Geotechnical Earthquake Engineering. Prentice Hall, Upper Saddle River, 653 pp.

Martin, T.E. (1999) Characterization of pore pressure conditions in upstream tailings dams. Proc. Tailings and Mine Waste '99, Fort Collins, Colorado, pp. 303-313.

Olson, S.M. & Mattson, B.B. (2008) Mode of shear effects on yield and liquefied strength ratios. Canadian Geotechnical Journal, p. 574-587.

Olson, S.M. (2001) Liquefaction Analysis of Level and Sloping Ground Using Field Case Histories and Penetration Resistance. Ph.D. Thesis, University of Illinois at Urbana-Champaign, Urbana III, 549 pp.

Olson, S.M. (2006) Liquefaction analysis of Duncan Dam using strength ratios. Canadian Geotechnical Journal, v. 43:5, p. 484-499.

Olson, S.M. & Stark, T.D. (2002) Liquefied strength ratio from liquefaction case histories. Canadian Geotechnical Journal, p. 629-647.

Olson, S.M. & Stark, T.D. (2003a) Use of laboratory data to confirm yield and liquefied strength ratio concepts. Canadian Geotechnical Journal, v. 40:6, p. 1164-1184.

Olson, S.M. and Stark, T.D. (2003b) Yield strength ratio and liquefaction analysis of slopes and embankments. ASCE Journal of Geotechnical and Geoenvironmental Engineering, v. 129:8, p. 727-737.

Pereira, E.L. (2005) Estudo do Potencial de Liquefação de Rejeitos de Minério de Ferro sob Carregamento Estático (Liquefaction Analysis of Iron Tailings Under Static Loading). Master Dissertation, Universidade Federal de Ouro Preto, Ouro Preto.

Pirete, W. (2010) Avaliação do Potencial de Liquefação Estática em Barragem de Rejeitos de Minério de Ferro com Base na Metodologia de Olson (Liquefaction Analysis of Iron Tailings Dams Using Olson Methodology). Master Dissertation, Universidade Federal de Ouro Preto, Ouro Preto.

Poulos, S.J.; Castro, G. & France, J.W. (1985) Liquefaction evaluation procedure. Journal of Geotechnical Engineering Division, ASCE, v. 111:6, p. 772-792.

Seed, H.B.; Tokimatsu, K.; Harder, L.F. & Chung, R. (1985) Influence of SPT procedures in soil liquefaction resistance evaluations. Journal of Geotechnical Engineering Division, ASCE, v. 111:12, p. 861-878.

Seid-Karbasi, M. & Byrne, P.M. (2004) Liquefaction, lateral spreading and flow slides. Proc. 57th Canadian Geotechnical Conf., Session 2c, pp. 23-30.

Sladen, J.A.; D'hollander, R.D. & Krahn, J. (1985) The liquefaction of sands, a collapse surface approach. Canadian Geotechnical Journal, p. 564-578.

Spencer, E. (1967) A method of analysis of the stability of embankments assuming parallel inter slice forces. Geotechnique, v. 17:1, p. 11-26.

Stark, T.D. & Mesri, G. (1992) Undrained shear strength of liquefied sands for stability analysis. Journal of Geotechnical Engineering, ASCE, v. 118:11, p. 1727-1747.

Troncoso, J.H. & Verdugo (1985) Silt content and dynamic behavior of tailings sands. Proc 11th ICSMFE, San Francisco, v. 3, pp. 131-1314

Vick, S.G. (1990) Planning, Design, and Analysis of Tailings Dams. 2nd edition. BiTech., Vancouver, 369 pp.

Yamamuro, J.A. & Lade, P.V. (1997) Effects of nonplastic fines on static liquefaction of sands. Canadian Geotechnical Journal, p. 918-928.

Yoshimi, Y.; Yanaka, K. & Tokimatsu, K. (1989) Liquefaction resistance of partially saturated sand. Journal of Soils and Foundations, v. 29:2, p. 157-162.